Marchesin et al., http://www.jcb.org/cgi/content/full/jcb.201506002/DC1

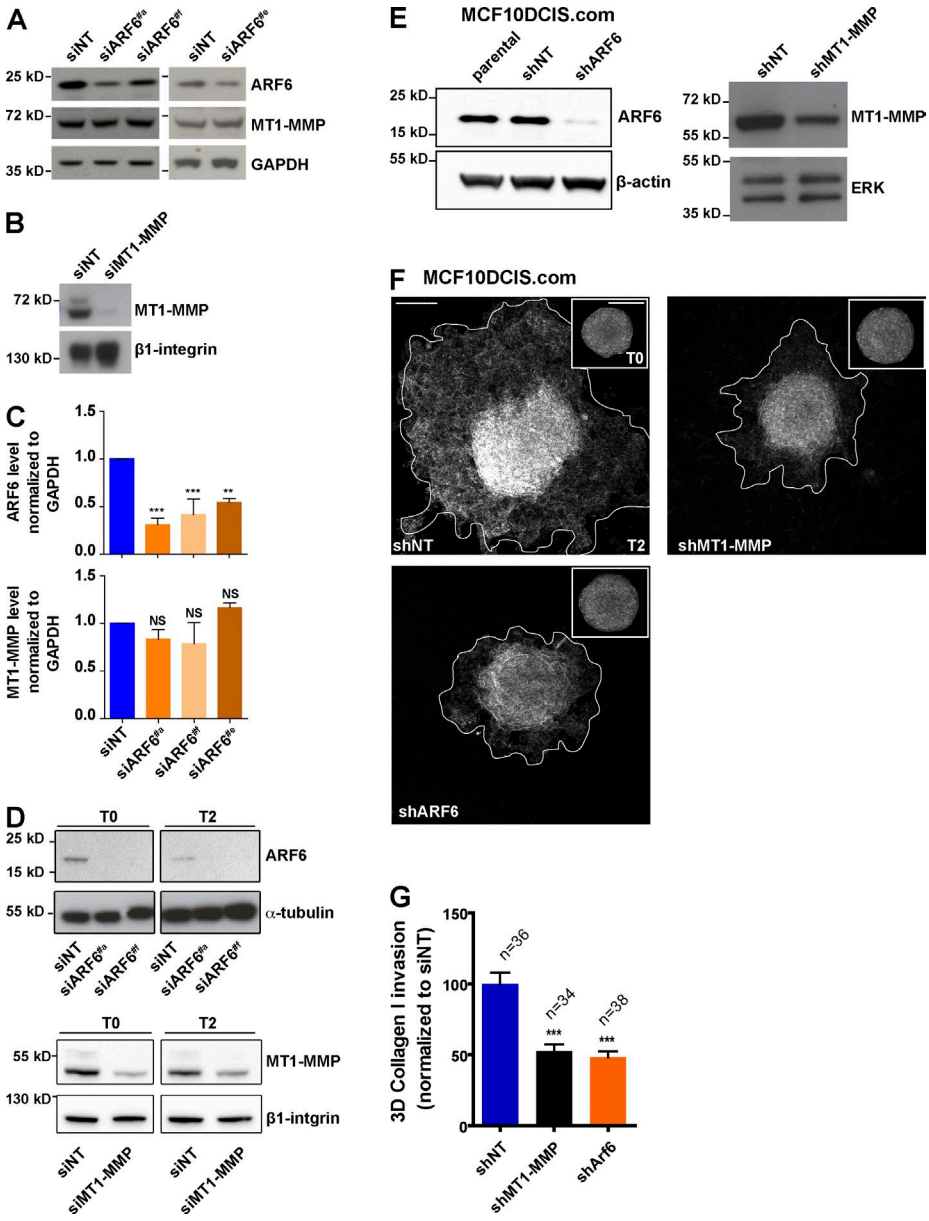

Figure S1. **ARF6 is required for invasion of MDA-MB-231 and MFCF10DCIS.com cells.** (A and B) Immunoblotting analysis of MDA-MB-231 cells treated with three independent siRNAs against ARF6 for 72 h using the indicated antibodies. (C) Quantification of protein expression in cells treated with siRNAs as in A. **, $P < 0.01$; ***, $P < 0.001$. (D) Protein levels in the different cell populations for multicellular spheroid assay were analyzed 72 (T0) and 120 h (T2) after siRNA treatments. Immunoblotting with anti–β-actin or anti–β1-integrin was used as a loading control. (E) Immunobloting analysis of MCF10DCIS.com cells stably knocked down for ARF6 or MT1-MMP expression by lentiviral shRNA expression. Immunoblotting with anti–β-actin or anti-ERK was used as a loading control. Antibody specificity is indicated on the right. (F) Phalloidin-labeled multicellular spheroids representative of each cell population collected after 2 d in 3D type I collagen (T2). Insets correspond to spheroids at T0. Bars, 200 µm. (G) Mean invasion area of spheroids at T2 normalized to the mean invasion area at T0 ± SEM and normalized to invasion of siNT spheroids. *n*, number of spheroids analyzed for each cell population. ***, $P < 0.001$ (compared with shNT multicellular spheroids).

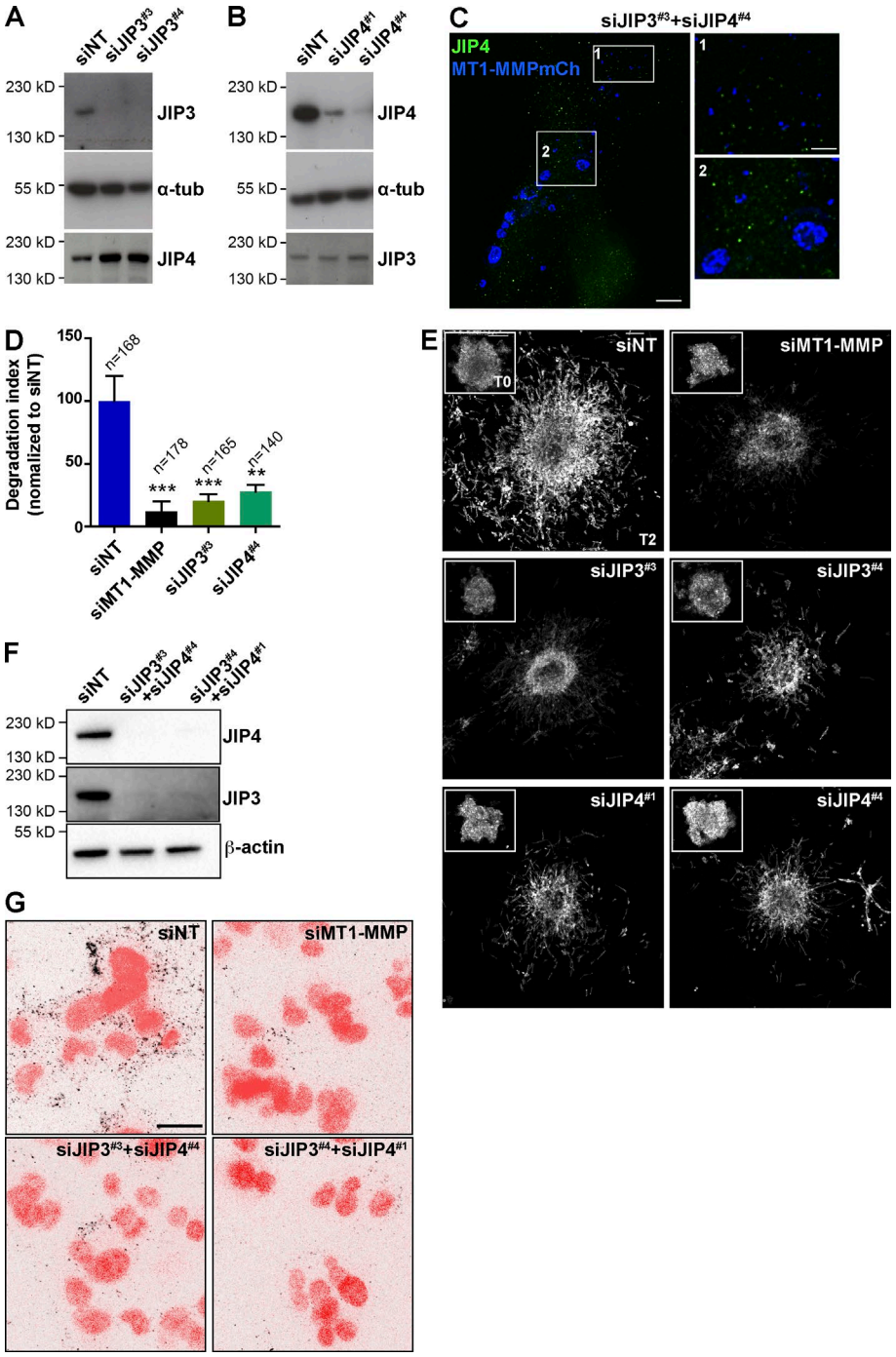

Figure S2. **JIP3 and JIP4 are required for gelatin degradation and invasive migration in 3D collagen.** (A and B) Immunoblot analysis of MDA-MB-231 cells knocked down for JIP3 or JIP4 after 72 h of siRNA treatment. Immunoblotting analysis with anti–α-tubulin was used as a loading control. (C) MDA-MB-231 cells expressing MT1-MMPmCh treated with the indicated siRNAs were seeded on gelatin, fixed, and stained for JIP4. Images are merged channels from deconvoluted z projections. Insets show higher magnification of boxed regions. Bars: 5 µm; (insets) 2 µm. (D) FITC-gelatin degradation index of MDA-MB-231 cells treated with the indicated siRNAs. Values are mean ± SEM. *n*, number of cells scored for each cell population. **, P < 0.01; ***, P < 0.001 (compared with siNT-treated cells). (E) Confocal images of phalloidin-labeled multicellular spheroids after 2 d in 3D collagen I gel. Insets correspond to spheroids at T0. Bars, 200 µm. (F) Immunoblot analysis of JIP3– and JIP4–knocked down MDA-MB-231 cells after 72 h of siRNA treatment. Immunoblotting analysis with anti–β-actin was used as a loading control. Antibody specificity is indicated on the right. (G) Confocal images of MDA-MB-231 cells treated with the indicated siRNAs embedded in type I collagen and stained for MT1-MMP–cleaved collagen (in black in the inverted image) and with DAPI (red). Bar, 20 µm.

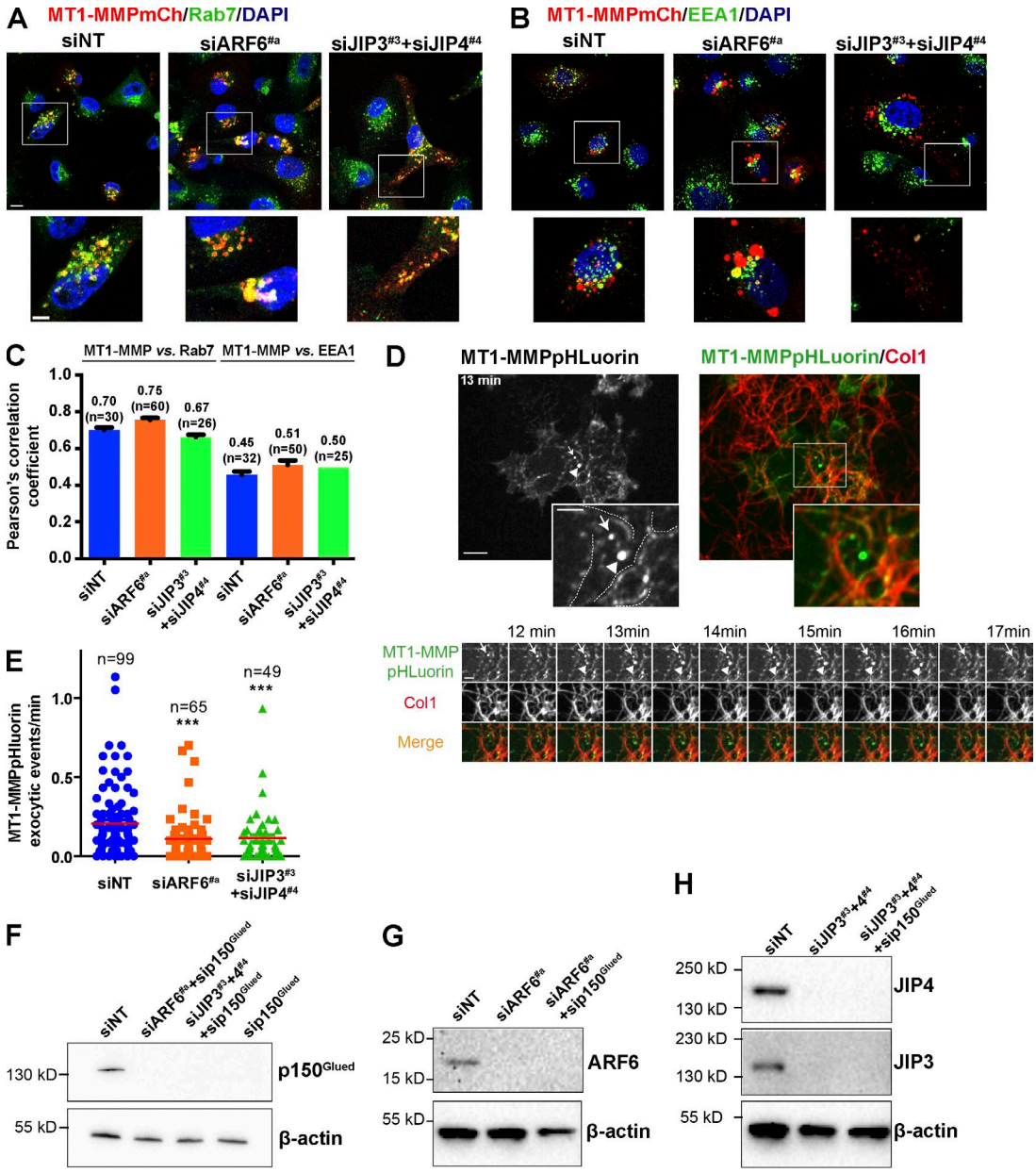

Figure S3. **ARF6 or JIP3/4 silencing does not affect colocalization of MT1-MMP and Rab7 on LEs but impairs MT1-MMP exocytosis.** (A and B) Confocal images of MDA-MB-231 cells stably expressing MT1-MMPmCh treated with the indicated siRNAs and plated on gelatin, fixed, and stained for DAPI, Rab7 (A), or EEA1 (B). Insets are higher magnification of the boxed regions. Bars: 10 µm; (insets) 5 µm. (C) Mean Pearson's correlation coefficient values ± SEM of MT1-MMP versus Rab7 or EEA1 markers in the different cell populations. *n*, number of cells analyzed. (D) Still image of a confocal spinning disk microscopy time-lapse sequence of MDA-MB-231 cells expressing MT1-MMPpHluorin (left panel and pseudocolored in green in merge image in right panel) plated on a layer of type I collagen fibers (red). Two exocytic flashes of MT1-MMPpHluorin are visible on the selected frame (pointed to by arrows and arrowheads). Insets are high magnification of the boxed region. MT1-MMPpHluorin accumulates along collagen I fibers (underlined by dashed lines). Bars: 10 µm; (insets) 5 µm. Gallery corresponds to the boxed region and shows exocytosis of MT1-MMPpHluorin–positive endosomes (arrows and arrowheads) in the vicinity of collagen I fibers. Bar, 5 µm. (E) MDA-MB-231 cells expressing MT1-MMPpHluorin silenced for the indicated proteins were seeded on a layer of type I collagen fibers and imaged over a 30-min time period. Frequency of MT1-MMPpHluorin exocytic events was quantified (box plots of events/cell/minute). *n*, number of cells analyzed for each cell population. ***, $P < 0.001$ (as compared with siNT-treated cells). (F–H) Immunoblotting analysis of MDA-MB-231 cells stably expressing MT1-MMPmCh treated with the indicated siRNAs. Antibody specificity is indicated on the right. Anti–β-actin was used as a loading control.

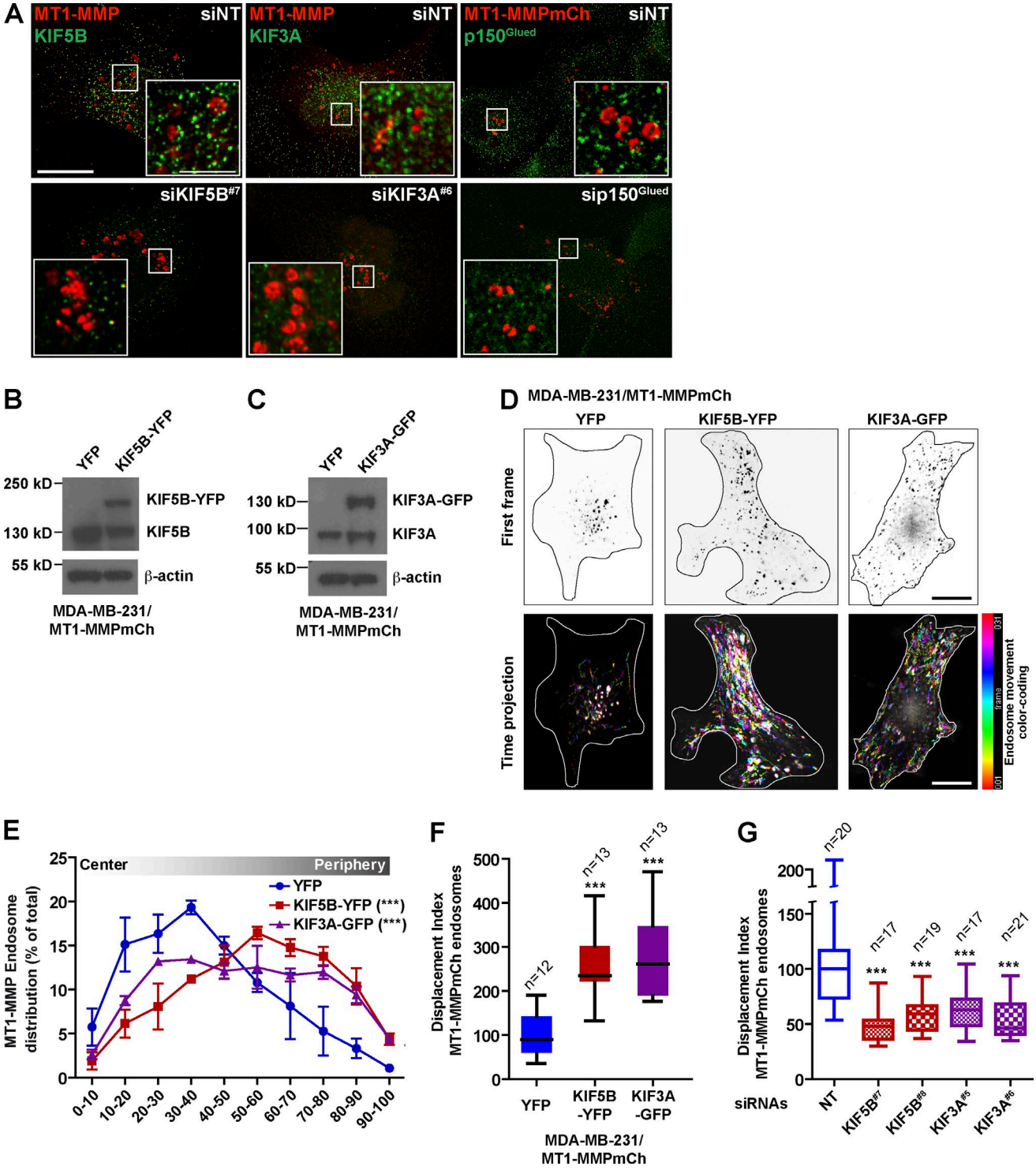

Figure S4. **KIF5B/kinesin-1 and KIF3A/kinesin-2 control MT1-MMP endosome motility and positioning.** (A) Specificity of IF staining by KIF5B (left), KIF3A (middle), or p150^{Glued} (right) antibodies was assessed by silencing the corresponding protein by siRNA treatment in MDA-MB-231 cells. MT1-MMP compartments were detected by endogenous staining or by expression of MT1-MMPmCh as indicated. Insets are high magnification images of the boxed regions. Bars: 5 µm; (insets) 1.3 µm. (B and C) Immunoblotting analysis of MDA-MB-231 cells stably expressing MT1-MMPmCh and KIF5B-YFP or KIF3A-GFP. Ectopic expression of YFP was used as a control. Immunoblotting with anti–β-actin was used as a loading control. (D) Inverted still image from confocal spinning disk microscopy time-lapse sequences showing MT1-MMPmCh–containing endosomes in cells treated with the indicated siRNA (top). Color-coded time projections of 31 consecutive time frames from these sequences (bottom, 2-s intervals). Color coding for time projections is shown on the right. Bars, 5 µm. (E) Automated quantification of intracellular distribution of MT1-MMPmCh–containing endosomes in cells stably expressing YFP, KIF5B-YFP, or KIF3A-GFP. Results are plotted as mean and SEM of the percentage of MT1-MMP–positive vesicles distributed according to the relative distance from the cell center to the cell periphery. ***, $P < 0.001$ (compared with YFP-expressing cells). (F and G) Displacement index of MT1-MMP–positive endosomes in the indicated cell populations was calculated by dividing the cellular area in which MT1-MMP endosomes had been present during the time lapse (maximum intensity projection generated from the 31 frames acquired with 2-s intervals) by the area that contained MT1-MMP endosomes in the first frame of the sequence. *n*, number of cells analyzed for each cell population. ***, $P < 0.001$ (compared with MT1-MMPmCh YFP-expressing cells in F or with siNT-treated cells in G).

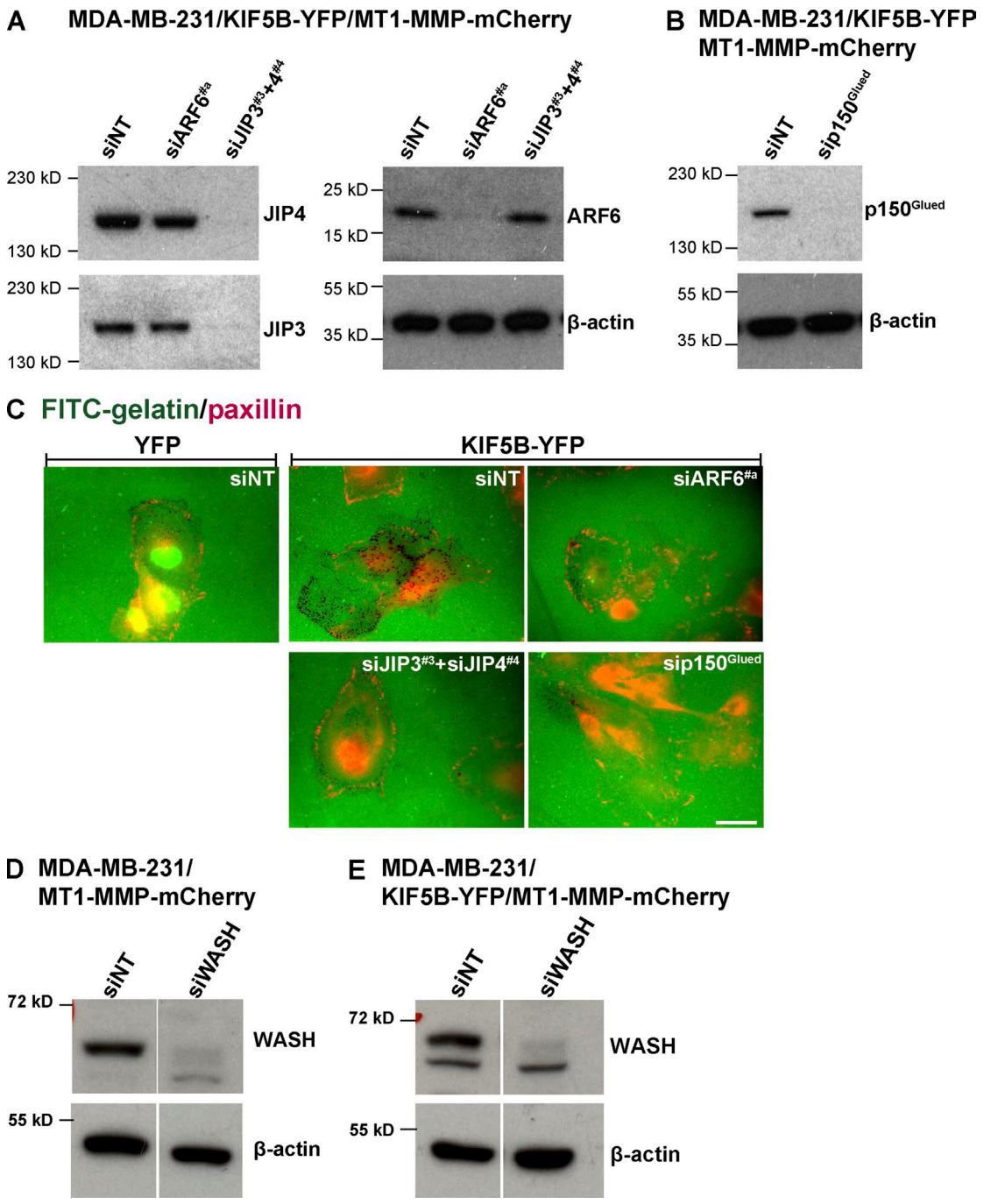

Figure S5. **Silencing of JIP3/JIP4, p150^{Glued}, or WASH interferes with stimulation of matrix degradation by KIF5B overexpression.** (A and B) Immunoblotting analysis of MDA-MB-231 cells stably expressing MT1-MMPmCh and KIF5B-YFP treated with the indicated siRNAs. Immunoblotting with anti–β-actin was used as a loading control. (C) Fluorescence images of the indicated cell populations plated on FITC-labeled gelatin (see Fig. 6 C). Bar, 5 µm. (D and E) Immunoblotting analysis of MDA-MB-231 cells stably expressing MT1-MMPmCh (D) or MT1-MMPmCh and KIF5B-YFP (E) treated with the indicated siRNAs. Anti–β-actin was used for equal loading.

Video 1. **ARF6 and JIP3/4 are required for correct positioning of MT1-MMPmCh–positive endosomes.** MDA-MB-231 cells stably expressing MT1-MMPmCh (inverted images, black) were treated with the indicated siRNAs, plated on glass-bottom dishes coated with cross-linked gelatin, and kept in a humidified atmosphere at 37°C and 1% CO_2. Images were analyzed by confocal spinning disk microscopy (1 z stack every 2 s for 3 min) using a spinning disk microscope. Bar, 20 µm.

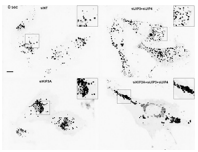

Video 2. **KIF3A is responsible for periphery positioning of MT1-MMP endosome in JIP3/JIP4-depleted cells.** MDA-MB-231 cells stably expressing MT1-MMPmCh (inverted images, black) were treated with the indicated siRNAs, plated on glass-bottom dishes coated with cross-linked gelatin, and kept in a humidified atmosphere at 37°C and 1% CO_2. Images were analyzed by confocal spinning disk microscopy (one z stack every 3 s for 3 min) using a spinning disk microscope. Insets are higher magnification views of the boxed regions. Bar, 10 µm.

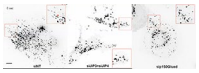

Video 3. **JIP3/4 and p150^{Glued} are required for MT1-MMPmCh–positive endosome tubulation.** MDA-MB-231 cells stably expressing KIF5B-YFP and MT1-MMPmCh (inverted images, black) were treated with the indicated siRNAs, plated on glass-bottom dishes coated with cross-linked gelatin, and kept in a humidified atmosphere at 37°C and 1% CO_2. Images were analyzed by confocal spinning disk microscopy (one z stack every 3 s for 3 min, with only ventral z stack images shown) using a spinning disk microscope. Insets are higher magnification views of the boxed regions. The red arrowheads point to elongating MT1-MMP endosomes. Bar, 10 µm.

Table S1. **Characteristics of primary tumors included in the TMA**

Characteristics	IDC *n* = 496
	(%)
Histological grade[a]	
I	83 (16.7)
II	154 (30.0)
III	258 (52.0)
Unknown	1 (0.2)
Histological subtype	
Ductal carcinoma	487 (98.2)
Lobular carcinoma	6 (1.2)
Others	3 (0.6)
Tumor size (cm)[b]	
T1 (<2)	330 (66.5)
T2 (2 NA 5)	148 (29.8)
T3 (>5)	14 (2.8)
T4	4 (0.8)
N stage[b]	
N0	272 (54.8)
N1	149 (30.0)
N2	55 (11.1)
N3	17 (3.4)
Unknown	3 (0.6)
ER status	
Positive	286 (57.7)
Negative	210 (42.3)
PR status	
Positive	255 (51.4)
Negative	241 (48.6)
HER2 status	
Positive	93 (18.7)
Negative	403 (81.3)
Ki67	
Positive (≥20%)	363 (74.0)
Negative (<20%)	133 (26.0)
Molecular subtype	
TNBC	131 (26.4)
HER2	79 (15.9)
Luminal A	147 (29.6)
Luminal B	139 (28.0)

Molecular subtypes were based on ER, PR, and HER2 status as described previously (Wolff et al., 2006; Prat et al., 2013; Rossé et al., 2014; Lodillinsky et al., 2015).
[a]Invasive breast cancers classified based on the Elston-Ellis classification system (grade I–III; Elston and Ellis, 1993).
[b]Based on TNM staging (Singletary et al., 2003). After IHC staining with anti-ARF6 antibodies, 426 IDC cases were available for scoring.

Table S2. **Comparison of membranous MT1-MMP and ARF6 and KIF5B and KI3A expression in breast cancer IDCs**

		ARF6 *n* (%)		KIF5B *n* (%)		KIF3A *n* (%)	
		Low	**High**	**Low**	**High**	**Low**	**High**
MT1-MMP	Low	168 (0.98)	3 (0.02)	65 (0.38)	106 (0.62)	17 (0.10)	154 (0.90)
	High	118 (0.84)	22 (0.16)	29 (0.21)	111 (0.79)	27 (0.19)	113 (0.81)
ARF6	Low	NA	NA	92 (0.32)	194 (0.68)	35 (0.12)	251 (0.88)
	High	NA	NA	2 (0.08)	23 (0.92)	9 (0.36)	16 (0.64)
KIF5B	Low	NA	NA	NA	NA	10 (0.11)	84 (0.89)
	High	NA	NA	NA	NA	34 (0.16)	183 (0.84)

311 IDCs. H-score variables were discretized either in low and high expression in order to perform association test. For MT1-MMP and ARF6, we used membranous H scores with a threshold estimated to 100. For KIF5B and KIF3A, total H scores (the sum of membranous and cytoplasmic IHC H scores) were used, and threshold was estimated to 200. NA, not applicable.

Table S3. **P-values of comparison of membranous MT1-MMP and ARF6 and KIF5B and KI3A expression shown in Table S2**

	P-values		
	ARF6	**KIF5B**	**KIF3A**
MT1-MMP	1.7×10^{-5}	0.001	0.03
ARF6	NA	0.02	0.004
KIF5B	NA	NA	0.32

H-scores were compared between groups by the chi-square test. NA, not applicable.

Table S4. **Antibodies used in this study**

Antibodies	**Type (species)**	**Source**
Arf6	Monoclonal (mouse)	EMD Millipore (clone 6ARF01)
JIP3	Polyclonal (rabbit)	Santa Cruz Biotechnology, Inc. (clone H-140)
JLP (JIP4)	Polyclonal (rabbit)	Abcam (ab12331)
MT1-MMP	Monoclonal (mouse)	EMD Millipore (clone MAB3328)
$p150^{Glued}$	Monoclonal (mouse)	BD Transduction Lab (clone 12/$P150^{Glued}$)
KIF3A	Polyclonal (rabbit)	Abcam (ab11259)
β-actin	Monoclonal (mouse)	Sigma-Aldrich (clone AC-15)
α-tubulin	Monoclonal (mouse)	Sigma-Aldrich (clone DM1A)
ERK	Polyclonal (rabbit)	EMD Millipore (06-182)
β1-integrin	Polyclonal (rabbit)	C. Albiges Rizo (Institut Albert Bonniot, Grenoble, France) Antigen: cytoplasmic domain
KIF5B (PCP42)	Polyclonal (rabbit)	R. Vale (University of California, San Francisco, San Francisco, CA) Antigen: aa 523–773 of uKHC
KIF5B	Monoclonal (mouse)	Covance (clone SUK-4)
Rab7	Monoclonal (rabbit)	Cell Signaling Technology (clone D95F2)
EEA1	Polyclonal (goat)	Santa Cruz Biotechnology, Inc. (clone N-19)
Cortactin	Monoclonal (mouse)	EMD Millipore (clone 4F11)
Paxillin	Monoclonal (mouse)	BD Transduction Lab (clone 349/Paxillin)
$Col1^{-3/4}C$	Polyclonal (rabbit)	ImmunoGlobe GmbH (0217-050)
WASH1	Polyclonal (rabbit)	Sigma-Aldrich (SAB4200372)
HRP-conjugated anti–rabbit IgG	Polyclonal (donkey)	Sigma-Aldrich (A0545)
HRP-conjugated anti–mouse IgG	Polyclonal (donkey)	Jackson ImmunoResearch Laboratories, Inc. (61871)

This table lists the primary and secondary antibodies used for this study and provides information regarding antibody species, antigen (homemade antibodies), and source.

Table S5. **siRNAs and shRNAs used for this study**

Gene	Sequence (Sens)	Company
siRNA		
ARF6#a	5′-CGGCAUUACUACACUGGGA-3′	Thermo Fisher Scientific
ARF6#e	5′-ACGUGGAGACGGUGACUUA-3′	Thermo Fisher Scientific
ARF6#f	5′-GCACCGCAUUAUCAAUGAC-3′	Ambion
MT1-MMP	5′-GGAUGGACACGGAGAAUUU-3′	Thermo Fisher Scientific
	5′-GGAAACAAGUACUACCGUU-3′	
	5′-GGUCUCAAAUGGCAACAUA-3′	
	5′-GAUCAAGGCCAAUGUUCGA-3′	
MAPK8IP3/JIP3#3	5′-GUUUGAAGAUGCUCUGGAA-3′	Thermo Fisher Scientific
MAPK8IP3/JIP3#4	5′-GAACAAAGCUUUCGGCAUC-3′	Thermo Fisher Scientific
SPAG9/JIP4#1	5′-GAGCAUGUCUUUACAGAUC-3′	Thermo Fisher Scientific
SPAG9/JIP4#4	5′-GCAUCACAGUGGUUGGUUG-3′	Thermo Fisher Scientific
DCTN1(p150^{Glued})	5′-CUGGAGCGCUGUAUCGUAA-3′	Thermo Fisher Scientific
	5′-GAAGAUCGAGAGACAGUUA-3′	
	5′-GCUCAUGCCUCGUCUCAUU-3′	
	5′-CGAGCUCACUACUGACUUA-3′	
WASH1	5′-UGUCGGAUCUCUUCAACAA-3′	Thermo Fisher Scientific
Nontargeting		Thermo Fisher Scientific
KIF5B#7	5′-CGGUCGUGAUCGCGUCCAATT-3′	QIAGEN
KIF5B#8	5′-GGCCGAGUGCAACAUCAAATT-3′	QIAGEN
KIF3A#5	5′-GACCUGAUGUGGGAGUUUATT-3	QIAGEN
KIF3A#6	5′-GGUUCAGAAAGACAGGCAATT-3′	QIAGEN
Exo84#d	5′-CACGGCTTTCTCATGAACGAT-3′	QIAGEN
shRNA		
Nontargeting	5′-CCGGCAACAAGATGAAGAGCACCAACTCGAGTTGGTGCTCTTCATCTTGTTGTTTTT-3′	Sigma-Aldrich
ARF6#2	5′-CCGGGTCAAGTTCAACGTATGGGATCTCGAGATCCCATACGTTGAACTTGACTTTTTG-3′	Sigma-Aldrich TRCN0000048003
MT1-MMP	5′-CCGGCGATGAAGTCTTCACTTACTTCTCGAGAAGTAAGTGAAGACTTCATCGTTTTTG-3′	Sigma-Aldrich TRCN0000050855

References

Elston, E.W., and I.O. Ellis. 1993. Method for grading breast cancer. *J. Clin. Pathol.* 46:189–190. http://dx.doi.org/10.1136/jcp.46.2.189-b

Lodillinsky, C., E. Infante, A. Guichard, R. Chaligné, L. Fuhrmann, J. Cyrta, M. Irondelle, E. Lagoutte, S. Vacher, H. Bonsang-Kitzis, et al. 2015. p63/MT1-MMP axis is required for in situ to invasive transition in basal-like breast cancer. *Oncogene.* http://dx.doi.org/10.1038/onc.2015.87

Prat, A., M.C. Cheang, M. Martín, J.S. Parker, E. Carrasco, R. Caballero, S. Tyldesley, K. Gelmon, P.S. Bernard, T.O. Nielsen, and C.M. Perou. 2013. Prognostic significance of progesterone receptor-positive tumor cells within immunohistochemically defined luminal A breast cancer. *J. Clin. Oncol.* 31:203–209. http://dx.doi.org/10.1200/JCO.2012.43.4134

Rossé, C., C. Lodillinsky, L. Fuhrmann, M. Nourieh, P. Monteiro, M. Irondelle, E. Lagoutte, S. Vacher, F. Waharte, P. Paul-Gilloteaux, et al. 2014. Control of MT1-MMP transport by atypical PKC during breast-cancer progression. *Proc. Natl. Acad. Sci. USA.* 111:E1872–E1879. http://dx.doi.org/10.1073/pnas.1400749111

Singletary, S.E., C. Allred, P. Ashley, L.W. Bassett, D. Berry, K.I. Bland, P.I. Borgen, G.M. Clark, S.B. Edge, D.F. Hayes, et al. 2003. Staging system for breast cancer: revisions for the 6th edition of the AJCC Cancer Staging Manual. *Surg. Clin. North Am.* 83:803–819. http://dx.doi.org/10.1016/S0039-6109(03)00034-3

Wolff, A.C., M.E. Hammond, J.N. Schwartz, K.L. Hagerty, D.C. Allred, R.J. Cote, M. Dowsett, P.L. Fitzgibbons, W.M. Hanna, A. Langer, et al. College of American Pathologists. 2006. American Society of Clinical Oncology/College of American Pathologists guideline recommendations for human epidermal growth factor receptor 2 testing in breast cancer. *J. Clin. Oncol.* 25:118–145. http://dx.doi.org/10.1200/JCO.2006.09.2775